04

RF cathode characteristics dependence on its design parameters

© A.M. Nikonov,[1] K.V. Vavilin,[1] I.I. Zadiriev,[1] S.A. Dvinin,[1] E.A. Kralkina,[1] G.V. Shvydkiy,[1] A.A. Golikov,[1] A.E. Sagalakov,[1] V.V. Sazonov,[1] A.S. Filatiev,[1] D.A. Bondarenko,[2] S.Yu. Marinin,[2] A.A. Khodov[2]

[1] Moscow State University,
119991 Moscow, Russia
[2] Joint Company Research and Production Corporation „Space Monitoring Systems, Information & Control and Electromechanical Complexes“ named after A.G. Iosifian,
107078 Moscow, Russia

e-mail: ekralkina@mail.ru

Received November 22, 2023
Revised January 10, 2024
Accepted January 14, 2024

The paper studies the characteristics of the RF model of an inductive cathode-neutralizer operating on argon and its mixture with air, when changing the design parameters of the device: the diameter of the output port and the area of the ion collector. It has been experimentally shown that the largest electron current can be obtained with an output port with a diameter of 2.2 mm and an ion collector of the largest area. Provided that the voltage between the ion collector and the anode is less than 100 V, under all the conditions considered, there is a slight drop in the electron concentration compared to a purely inductive discharge in the cathode, at the same time the electron current to the anode increases greatly. The interpretation of the obtained results is carried out under the assumption that the discharge between the cathode and the anode is a combination of an inductive RF discharge and a DC discharge.

Keywords: neutralizer cathode, inductive radio frequency discharge, plasma, ions, electron current.

DOI: 10.61011/JTF.2024.04.57531.291-23

Introduction

In recent years, the feasibility of spacecraft (SC) operation in very low near-Earth orbits (120−250 km), which opens up new opportunities for monitoring of the surface of planets, communications, and ionospheric studies, has been discussed extensively in literature [1]. A considerable aerodynamic drag felt by spacecraft in such orbits poses a problem for their maintenance. Electric propulsion (EP) engines, which have an order of magnitude greater specific impulse than liquid propellant engines and provide an opportunity to reduce significantly the necessary fuel reserve, are advantageous in this context. A dramatic reduction of the needed reserve may be achieved with air-breathing electric propulsion (ABEP) engines by using residual gases in the surrounding atmosphere as a propellant.

It follows from the results of analysis of prerequisites for maintenance of SC with ABEP engines in very low near-Earth orbits [2] that the exit velocity of gases leaving ABEP engines should exceed 25 km/s. At present, such velocities are achieved only in flight models of ion engines (with an ion-optical acceleration system). Experimental studies into the operation of atmosphere-breathing ion engines have been performed in the last decade [2]. One of the problems arising in the construction of an ABEP engine is the need to ensure long-term operation of its systems in a medium containing a considerate fraction of chemically active atomic oxygen. Non-conventional solutions may be required in this context. Specifically, the ways to neutralize an ion jet at the ABEP engine exit should be examined. Incandescent and arc hollow cathodes are used for this purpose in modern EP engines [3–6]. A short lifetime, which decreases significantly when chemically active gases are mixed with an inert propellant gas, is their major drawback [4]. It was demonstrated in [7–18] that cathodes with an electrodeless inductive radio-frequency (RF) discharge may serve as alternatives to traditional devices. They have a considerable advantage over electrodeless cathodes with capacitive RF and microwave discharges in providing an opportunity to maintain a needed electron current with a lower energy consumption [11].

The model of physical processes within an RF inductive cathode proposed in [7] underlies the design of modern cathodes of this kind. It is assumed that power introduced into a discharge in the course of RF current flow through an inductor induces the formation of dense plasma within a cathode. Constant voltage is applied between a special metallic electrode (ion collector) in the cathode and the anode positioned outside the cathode. This voltage facilitates the extraction of electrons from the bulk of the cathode into the space between the cathode and the anode via a special port in the end face of the cathode. It is assumed that propellant gas does not become ionized in the space between the cathode and the anode. The extracted electron current should be equal to the ion current to the collector. In view of this, engineers designing RF cathodes

make every effort to maximize the ion collector area. A numerical model of a discharge was developed in [7], and key characteristics of the cathode were calculated. The results obtained this way are close to the experimental ones.

1. Application of an RF cathode in an ABEP engine

The environment conditions in which the RF cathode is to be operated as a part of an ABEP engine and the key requirements for the cathode may be determined by analyzing possible closed SC orbits and engine parameters needed to maintain them. A method for optimizing the parameters of spacecraft, ABEP engines, and elliptical SC orbits with respect to the peak power demand of an ABEP engine was presented in [19]. The dependences of optimum perigee height and power demand on the minimum admissible gas concentration in the ionization chamber of an ABEP engine, which were calculated using this method, are shown in Fig. 1. These dependences were obtained for spacecraft with cross-section area $A_{\text{in}} = 0.04\,\text{m}^2$, atmospheric parameters corresponding to a moderate solar activity according to ISO/FDIS 14222 [20], and thrust engine efficiency $\eta_T = 0.4$.

The results of experimental studies of air-breathing ion engines (IEs) [2] revealed that stable burning of plasma (even in radio-frequency IEs) is achieved at gas concentration $n \geq 8 \cdot 10^{18}\,\text{m}^{-3}$ in the ionization chamber. At $n_{\text{adm}} = 8 \cdot 10^{18}\,\text{m}^{-3}$, the pressure of surrounding atmosphere at the optimum elliptical orbits of spacecraft with ABEP engines does not exceed $2 \cdot 10^{-5}$ Torr.

Ion beam current I_b, which is to be neutralized using the RF cathode, may be determined with consideration of gas intake efficiency $\eta_c = 0.4$ determined in [19], known concentration of atmospheric molecules $n_\infty = 1.52 \cdot 10^{17}\,\text{m}^{-3}$,

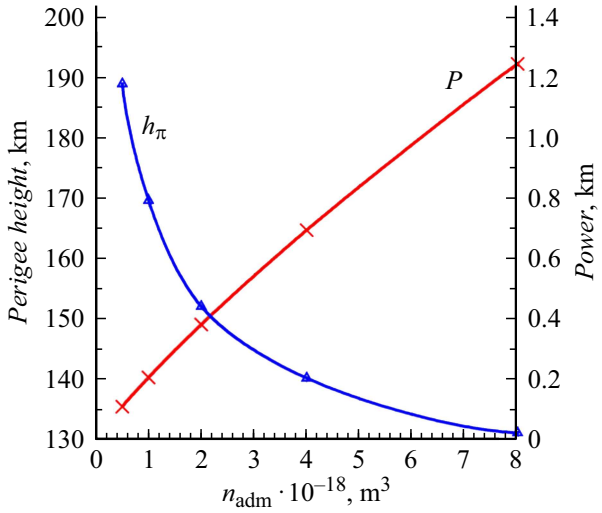

Figure 1. Dependences of optimum perigee height h_π and power demand W on minimum admissible gas concentration n_{adm} in the ionization chamber of an ABEP engine.

and accelerating potential $U = 1500\,\text{V}$ from the formulae given in [5]:

— the thrust of an ABEP engine is

$$F = I_b \sqrt{2\frac{M}{e}U},$$

where e is the electron charge and M is the molecular mass of atmospheric gases;

— the mass flow through an ABEP engine is

$$\dot{m} = \eta_c \cdot M n_\infty V A_{\text{in}},$$

where $V = 8049\,\text{m/s}$ is the SC velocity at the perigee of an elliptical orbit ($h_\pi = 130\,\text{km}$, $h_\alpha = 930\,\text{km}$);

— the power demand of an ABEP engine is

$$W = \frac{F^2}{2\dot{m}\eta_T}.$$

Hence, we find

$$I_b = \sqrt{\frac{W n_\infty e \cdot A_{\text{in}} V \eta_c \eta_T}{U}}.$$

With the above parameter values factored in,one may determine that the RF cathode for an ABEP engine at $n_{\text{adm}} = 8 \cdot 10^{18}\,\text{m}^{-3}$ should be targeted at neutralizing an ion beam with current $I_b = 1.0\,\text{A}$.

2. Experimental setup and measurement procedure

We have performed the first experimental studies of parameters of a cathode-neutralizer operating based on an inductive RF discharge in argon in [18]. The examined ranges of argon flow rate and RF generator power were 4–10 cm^3/min and 35–150 W, respectively. The obtained results confirmed the viability of the developed cathode model. In the present study, the examination of characteristics of an RF cathode utilizing argon and its mixture with air is continued. The influence of the cathode output port diameter and the ion collector area on the parameters of the RF cathode model is analyzed, and the necessity of refinement of the model of physical processes in the cathode is advocated.

A vacuum chamber 0.8 m^3 in volume, which was evacuated with a system of forevacuum and turbomolecular pumps, was used to measure the RF cathode parameters. The residual pressure in the vacuum chamber was on the order of 2.10^{-5} Torr. In the process of RF cathode operation, the pressure in the chamber did not exceed 4.10^{-4} Torr.

The RF cathode is a cylindrical gas-discharge chamber (GDC) with two metallic flanges. Its side walls are fabricated from a dielectric material. The chamber diameter and length are 30 and 80 mm, respectively. A metallic electrode (ion collector) is located within the GDC. The ion collector is a system of 16, 8, or 2 copper rods 2 mm

in diameter and 70 mm in length positioned at a distance of 12 mm from the cathode axis. The gas inlet needed to introduce propellant gas into the cathode is at the bottom flange of the chamber. The output port is on the axis of the top flange. Flanges with ports with diameter d of 2.2, 3, and 5 mm were used in the present study. A metallic electrode (anode) is mounted at a distance of 50 mm from the cathode.

A solenoidal 5-turn antenna inducing an inductive RF discharge is positioned on the side surface of the cathode. In order to ignite and maintain an inductive RF discharge within the GDC, the ends of this antenna are connected via a matching system to an RF generator with an operating frequency of 13.56 MHz and power P_{gen} that may be adjusted within the 0–1000 W range. Constant voltage V is applied between the ion collector and the anode after the ignition of a discharge. Ballast resistance $R = 100\,\Omega$ is introduced into the circuit between the electrodes. Voltage U_d between the cathode and the anode is then written as $U_d = V - IR$. The used power source allows one to measure currents up to 1.5 A.

A compensated Langmuir probe 4 mm in length and 0.37 mm in diameter was used to determine the parameters of plasma within the cathode. The probe was positioned at a distance of 7 mm from the cathode axis. Plasma parameters were calculated using the standard procedure for processing of probe characteristics. The electron temperature was determined from the slope of the dependence of logarithm of the electron current to the probe on the probe potential near the space potential.

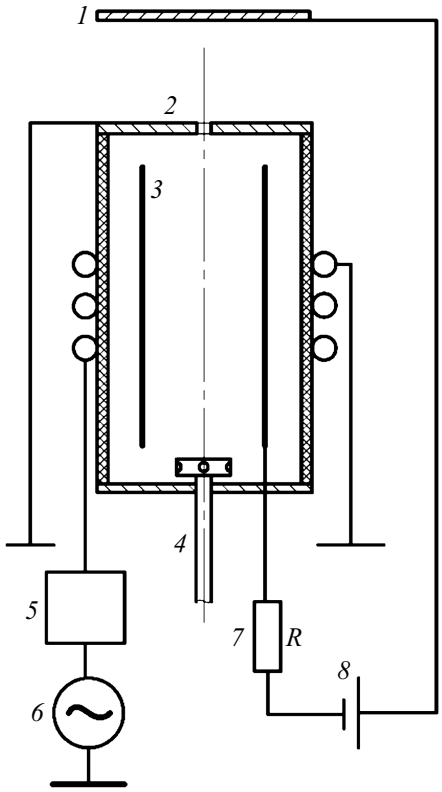

Figure 2. Diagram of the experimental RF cathode and its electrical circuit: *1* — electron collector, *2* — cap with an output port, *3* — ion collector, *4* — gas inlet, *5* — matching device, *6* — RF generator, *7* — ballast resistance, and *8* — constant-voltage source.

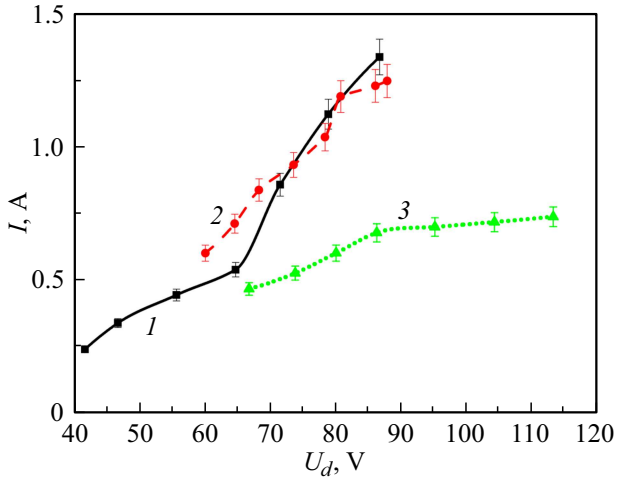

Figure 3. Dependence of electron current to the anode on the potential difference between the ion collector and the anode in RF cathode models with the following output port diameter: *1* — 2.2, *2* — 3, and *3* — 5 mm. The argon flow rate is 8 cm^3/min. $P_{gen} = 80$ W.

Argon with flow rate $f = 4$–10 cm^3/min and its mixture with air were used as a propellant. The air flow rate was varied within the 1–2 cm^3/min range. The cathode–anode voltage was varied from 0 to 160 V (Fig. 2).

3. Experimental results

Experiments revealed that the discharge at low argon flow rates (f below 5 cm^3/min), moderate RF generate power levels (P_{gen} below 80 W), and all the examined voltages U_d between the ion collector and the anode is concentrated within the RF cathode, and electron current I to the anode is zero. At $f > 5$ cm^3/min, current emerges in the circuit between the ion collector and the anode.

The dependence of I on voltage U_d measured at a flow rate of 8 cm^3/min and an RF generator power of 80 W is shown in Fig. 3.

It can be seen that the values of electron current corresponding to output port diameters of 2.2 and 3 mm are matching within the measurement accuracy in the U_d range of 55–85 V. The values of electron current measured in experiments with $d = 5$ mm turned out to be significantly lower than the values for smaller output port diameters. Conspicuous is the fact that curve $I(U_d)$ for $d = 5$ mm tends to saturation, differing in this respect from dependences $I(U_d)$ measured at $d = 2.2$ and 3 mm, which increase rapidly with U_d.

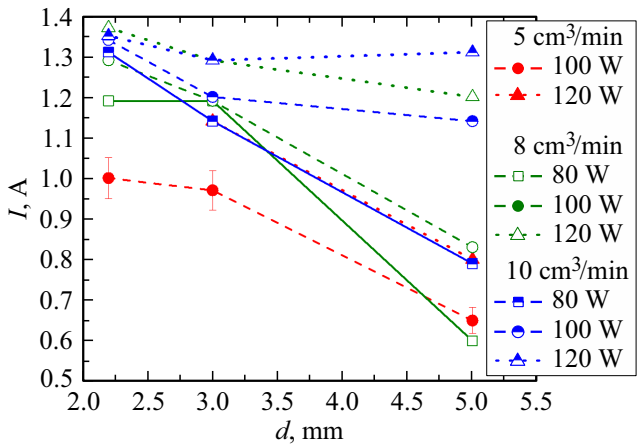

Figure 4. Dependences of electron current on the output port diameter obtained at $U_d = 80$ V; RF generator power of 80, 100, and 120 W; and argon flow rate of 5, 8, and 10 cm^3/min.

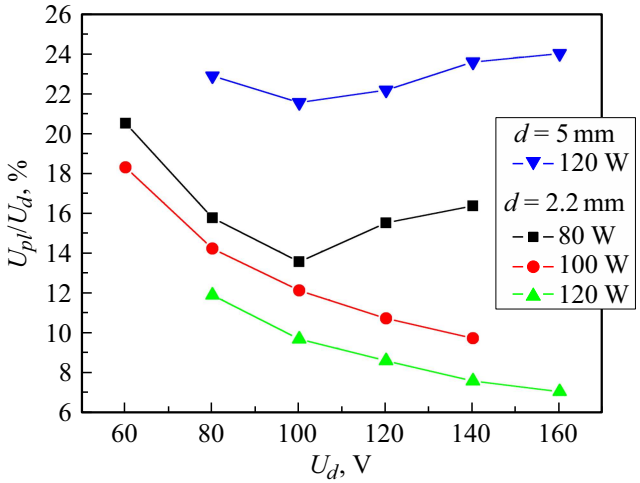

Figure 5. Dependence of ratio U_{pl}/U_d between plasma potential U_pl within the cathode and the voltage between the ion collector and the anode on U_d.

Figure 4 presents the dependences of electron current on the output port diameter obtained at $U_d = 80$ V and various power levels and argon flow rates.

It is evident that the electron current decreases with increasing port diameter in all the examined cases. However, dependence $I(d)$ becomes much less pronounced as power P_{gen} grows at flow rates of 8 and 10 sccm. Specifically, the difference in I values is on the order of 5% at $f = 10$ sccm.

Figure 5 presents the variation of ratio U_{pl}/U_d between plasma potential U_{pl} within the cathode and the voltage between the ion collector and the anode with U_d.

The data in Fig. 5 suggest that only a small fraction of potential difference (no greater than 25%) between the ion collector and the anode falls within the RF cathode. At an RF generator power of 80 W and an output port diameter of 2.2 mm, the dependence of U_{pl}/U_d on U_d is nonmonotonic with a minimum at $U_d \sim 100$ V, where U_{pl} is the potential of plasma in the cathode. As P_{gen} increases, the local minimum in the examined U_d range vanishes. The higher the generator power is, the lower are the values of ratio U_{pl}/U_d. When the port diameter increases to 5 mm, the dependence of U_{pl}/U_d on U_d is nonmonotonic even at $P_{gen} = 120$ W.

Figures 6, 7 present the variation of temperature T_e and the ratio between concentration n_e of electrons within the cathode and the corresponding value measured in a purely inductive discharge ($U_d = 0$) with voltage applied between the ion collector and the anode.

A reduction in electron concentration in the cathode and an increase in electron temperature are observed at $U_d > 100$ V in all the examined cases. It should be noted that the concentration and temperature of electrons within the cathode vary only slightly at $U_d < 100$ V, while the electron current to the anode increases.

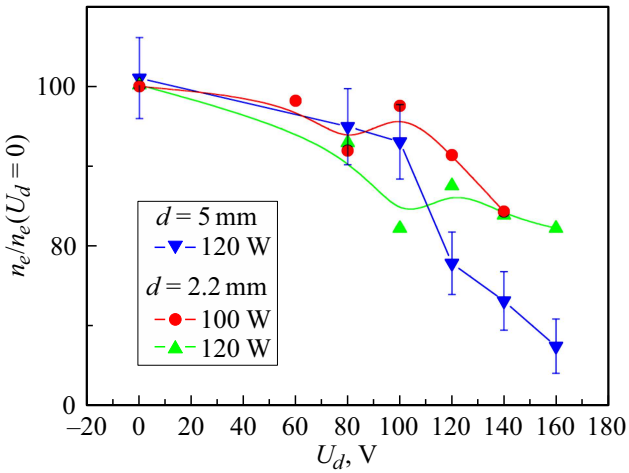

Figure 6. Dependence of ratio $n_e(Ud)/n_e(U_d = 0)$ between the electron concentration within the cathode and the concentration measured at $U_d = 0$ on U_d.

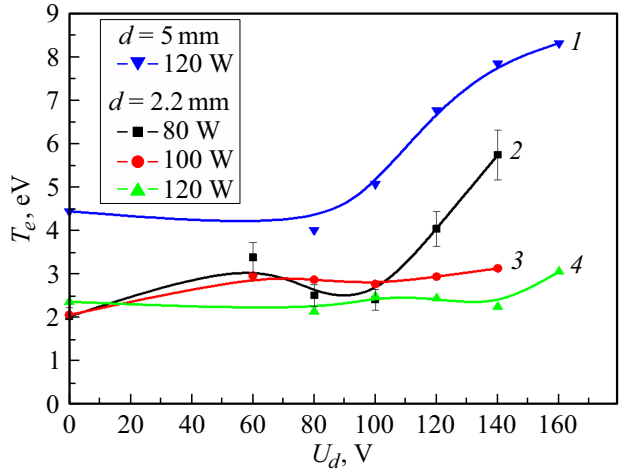

Figure 7. Dependence of the electron temperature within the cathode on voltage U_d between the ion collector and the anode.

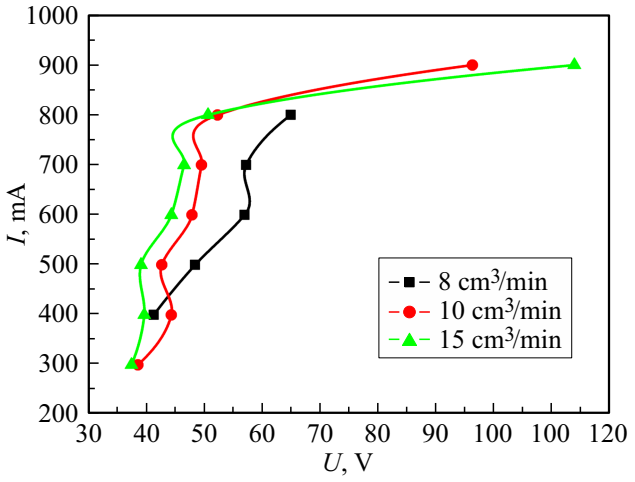

Figure 8. Dependence of electron current to the anode on the voltage between the cathode and the anode, $d = 2.2$ mm.

Figure 8 presents the typical $I(U_d)$ dependence obtained with the use of an ion collector made of 16 copper rods. It is evident that the electron current reaches saturation at a low RF generator power (50 W). At high P_{gen} values, no saturation region is found within the examined range of electron currents.

With eight copper rods serving as a collector, electron current saturation is also observed at $P_{gen} = 50$ W; notably, the maximum I value obtained with 8 rods (I_8) was 1.4 times lower than the one corresponding to 16 rods (I_{16}; see Fig. 9). An increase in RF generator power induced an intriguing effect: the $I(U_d)$ dependence became double-valued. At first, I_8 lags behind I_{16}, but then I_8 starts increasing and gets close to I_{16}, while the cathode–anode potential difference decreases.

When two copper rods were used as a cathode, only the model with a 5 mm port produced electron current; notably, more than 90% of voltage applied between the cathode and the anode fell near the ion collector.

The influence of admixed air on the $I(U_d)$ dependences was examined last. The obtained results are shown in Fig. 10. It is evident that the electron current decreases by no more than 10% if 1 cm^3/min of air are fed into the discharge; however, the electron current decreases by a factor of 2 as a result of a two-fold enhancement of the indicated flow rate. When pure air was used as a propellant gas, no electron current could be detected.

4. Discussion

In order to interpret the obtained results, we consider a discharge burning between the cathode and the anode as a combination of an inductive RF discharge and a DC discharge. Power is introduced into this discharge via both RF and DC channels. It seems reasonable to distinguish several sections of a combined discharge. The first section is the plasma region within the cathode, the second one is the region of a high electron current density near the cathode output port, and the third section is the plasma region in the gap between the cathode and the anode. The results of probe measurements revealed that the potential drop near the ion collector is marginal when a large-area ion collector is used. It is natural to assume that the potential drop is largely concentrated around the cathode output port. Electrons here are accelerated by a potential difference emerging between the first and third discharge sections. The electron energy is sufficient for gas ionization in the third discharge region. The number of electrons flowing from the cathode to the gap between the cathode and the anode depends largely on power introduced into the discharge via the inductive channel and on the electron concentration in the cathode.

In order to find whether gas ionization between the cathode and the anode is possible, we estimate the density of atoms in different sections of the discharge. Atom concentration n_0 within the cathode is estimated by equating the flux of atoms entering the cathode to the flux of atoms leaving through the output port with a thermal velocity. Assuming that the gas temperature is 100°C and the argon flow rate is 10 cm^3/min, we find that n_0 is 1, 0.5, and $0.2 \cdot 10^{16}$ cm^{-3} for output port diameters of 2.2, 3, and 5 mm. A rough estimate of the concentration of atoms in the gap between the cathode and the anode is obtained under the assumption that n_0 decreases here in proportion to the distance from the cathode output port squared. It follows that n_0 decreases by more than 3 orders of magnitude near the anode; therefore, the ionization rate near the anode is low. However, the concentration of atoms at a distance of 1–2 cm from the cathode output port is sufficiently high, and the process of ionization of atoms by accelerated electrons may proceed at a high rate. The electron current to the anode then increases due to the production of secondary electrons in the third discharge section. The ion current from the third discharge section to the first one also increases.

Let us examine the results of experiments with this pattern of physical processes in mind. An increase in cathode–anode voltage in the $U_d < 100$ V range leads to a reduction in U_{pl}/U_d (fraction of potential that falls near the ion collector). The electron concentration and temperature remain unchanged within the measurement accuracy. When the RF generator power increases, U_{pl}/U_d decreases; at the same time, the plasma concentration varies only slightly, while the electron temperature goes down. The magnitude of T_e reduction increases with RF generator power. It should be stressed that the electron current to the anode grows rapidly in the $U_d < 100$ V region. This is an indicator of significance of processes in the second and third discharge sections. At $U_d > 100$ V, a generator power of 80 W, and $d = 5$ mm, U_{pl}/U_d starts growing. An increase in the potential drop near the ion collector leads to acceleration of the flux of electrons emitted from the collector as a result of ion-electron emission and to intensification of the ionization process within the cathode.

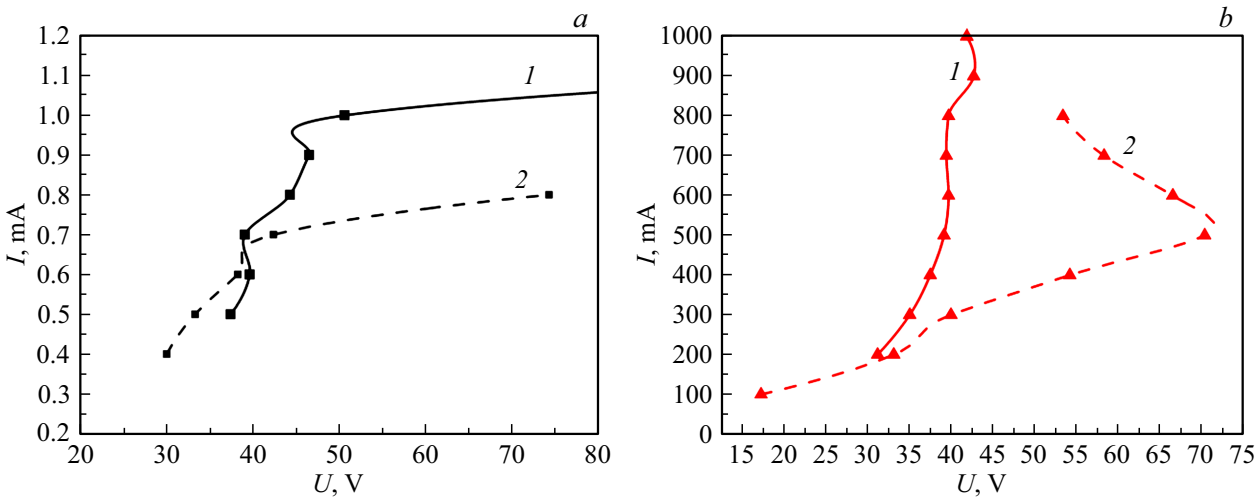

Figure 9. Dependence $I(U_d)$ measured with 16 (solid curve *1*) and 8 (dashed curve *2*) rods serving as an electron collector: *a* — 50, *b* — 100 W; $d = 2.2$ mm.

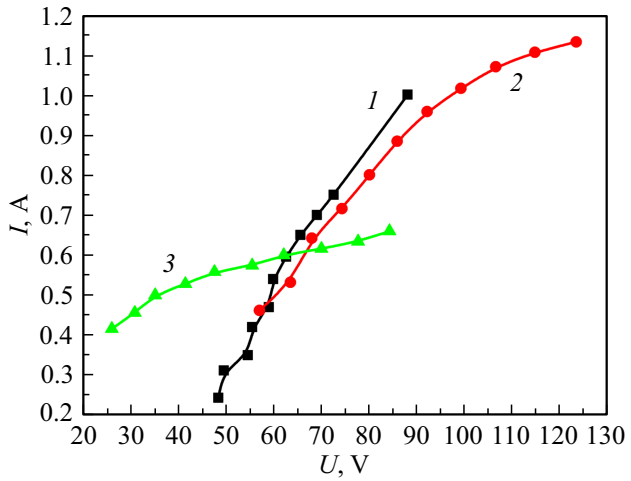

Figure 10. Dependence $I(U_d)$ measured in pure argon and in a mixture of argon and air. The argon flow rate is 5 cm^3/min in all cases. *1* — Pure argon; *2* — mixture of argon and air, the air flow rate is 1 cm^3/min; *3* — mixture of argon and air, the air flow rate is 2 cm^3/min.

When the port diameter increases, the concentration of atoms within the cathode decreases. This is accompanied by an increase in U_{pl}/U_d and the extension of influence of the DC channel. The concentration of neutrals increases with increasing gas flow rate, and the electron current to the anode becomes almost independent of the port diameter.

The dependence of electron current to the anode presented in Figs. 8, 9, *a* has a shape typical of CVCs of a non-self-sustained DC discharge [21]. The RF power introduced into the cathode serves as the source of additional ionization. The rapidly growing section of curve $I(U_d)$ corresponds to those conditions under which electrons produced within the cathode as a result of introduction of RF power reach the anode under the influence of voltage applied between the collector and the anode. When almost all charges produced within the cathode escape to the anode, the electron current reaches saturation. The current may grow only via an increase in the potential drop near the ion collector and intensification of ionization due to processes typical of a DC discharge. An increase in argon flow rate and RF generator power is accompanied by the growth of ionization rate due to effects typical of an inductive RF discharge.

It is known that an inductive discharge is ignited and burns in the capacitive mode at low P_{gen} values. It was demonstrated in [22] that the presence of a DC channel induces a reduction in threshold values of P_{gen} at which a discharge goes over from the capacitive mode to the inductive one. The higher the fraction of power introduced into a discharge via a DC channel is, the sooner does this transition occur. A reduction in the cathode area due to the use of fewer rods in the ion collector is accompanied by a reduction of power introduced into a discharge via a DC channel. The transition to the inductive mode is slowed down in this case. Following the transition of a discharge in the cathode to the inductive mode, the electron current rises steeply, the potential drop across the ballast resistance increases, and U_d decreases. This provides an explanation for the double-valued nature of curve $I(U_d)$ measured with an ion collector made of eight rods.

It is known [22] that when argon is substituted with air (with external parameters of an inductive RF discharge remaining unchanged), the plasma density decreases and the region of transition from the capacitive mode to the inductive one shifts along the generator power scale. The reduction in electron current to the anode observed after the mixing of argon with air is apparently attributable to the influence of both indicated factors.

Let us use the data presented in Fig. 4 to estimate cathode gas efficiency γ:

$$\gamma = i_e/(\text{eff})$$

and the power consumption for production of electron current with a strength of 1 A:

$$C_e = V_{ca} + P_{gen}/i_e.$$

These estimates demonstrate that the power consumption for the model with port diameter $d = 2.2$ mm is 140 W/A at $\gamma = 2.8$, which is close to the best current results [7].

Conclusion

The characteristics of a model of an RF inductive cathode-neutralizer utilizing argon and its mixture with air were examined under variation of the following design parameters of the device: the output port diameter and the ion collector area. It was demonstrated experimentally that the electron current is maximized when the port diameter is 2.2 mm and the ion collector area is the highest. Probe measurements demonstrated that only a small fraction of potential difference (no greater than 25%) between the ion collector and the anode falls within the RF cathode. At an RF generator power of 80 W and an output port diameter of 2.2 mm, the dependence of U_{pl}/U_d on voltage U_d between the ion collector and the anode is nonmonotonic with a minimum at $U_d \sim 100$ V. When the RF generator power increases, the local minimum vanishes. When the port diameter increases to 5 mm, the dependence of U_{pl}/U_d on U_d is nonmonotonic even at $P_{gen} = 120$ W. In all the examined cases, the electron concentration reduction at $U_d < 100$ W is small compared to a purely inductive discharge in the cathode; at the same time, the electron current to the anode increases significantly. The obtained results were interpreted under the assumption that a discharge between the cathode and the anode is a combination of an inductive RF discharge and a DC discharge.

The smallness of the potential drop near the ion collector gives reason to believe that its sputtering should have a negligible influence on the service life of an RF cathode.

Estimates revealed that the power consumption for the model with port diameter $d = 2.2$ mm is 140 W/A at $\gamma = 1.9$ and 180 W/A at $\gamma \sim 1$, which is close to the best results reported in literature.

Funding

This study was carried out under the program for support of interdisciplinary research and education schools of the Moscow State University, agreement No. 23-Sh01-02.

Conflict of interest

The authors declare that they have no conflict of interest.

References

[1] A.S. Filatyev, O.V. Yanova. Acta Astronautica, **158**, 23 (2019). DOI: 10.1016/j.actaastro.2018.10.039

[2] A.S. Filatyev, A.A. Golikov, A.I. Erofeev, S.A. Khartov, A.S. Lovtsov, D.I. Padalitsa, V.V. Skvortsov, O.V. Yanova. Progr. Aerospace Sci., **136**, 100877 (2023). DOI: 10.1016/j.paerosci.2022.100877

[3] H.R. Kaufman, R.S. Robinson. *Operation of Broad Beam Sources* (Commonwealth Scientific, Alexandria, 1984)

[4] D.M. Goebel, I. Katz. *Fundamentals of Electric Propulsion: Ion and Hall Thrusters* (JPL Space Science and Technology Series, California, 2008)

[5] O.A. Gorshkov, V.A. Murav'ev, A.A. Shagaida, A.S. Koroteev. *Khollovskie i ionnye plazmennye dvigateli dlya kosmicheskikh apparatov* (Mashinostroenie, M., 2008) (in Russian).

[6] S. Mazouffre. Plasma Sources Sci. Technol., **25**, 033002 (2016). DOI: 10.1088/0963-0252/25/3/033002

[7] F. Scholze, B.M. Tartz, H. Neumann. Rev. Sci. Instrum., **79**, 02B724 (2008). DOI: 10.1063/1.2802587

[8] S. Jahanbakhsh, M. Satir, M. Celik, Rev. Sci. Instrum., **87**, 02B922 (2016). DOI: 10.1063/1.4935015

[9] P. Dietz, F. Beckery, K. Keib, K. Holstev, P.J. Klar. In *Proceedings of International Electric Propulsion Conference* (Vienna, 2019), p. 207.

[10] F. Scholze, D. Spemann, D. Feili. In *Proceedings of International Electric Propulsion Conference* (Ann Arbor, 2009), p. 475.

[11] P. Smirnov, M. Smirnova, J. Schein, S. Khartov. In *Proceedings of International Electric Propulsion Conference* (Vienna, 2019), p. 840.

[12] T. Hatakeyama, M. Irie, H. Watanabe, A. Okutsu, J. Aoyagi, H. Takegahara. In *Proceedings of International Electric Propulsion Conference* (Florence, 2007), p. 226.

[13] V. Godyak, Y. Raitses, N.J. Fisch. In *Proceedings of International Electric Propulsion Conference* (Florence, 2007), p. 266.

[14] S. Weis, K.H. Schartner, H. Lob, D. Feili. In *Proceedings of International Electric Propulsion Conference* (Princeton, 2005), p. 86.

[15] B.W. Longmier, N. Hershkowitz. In *41st AIAA Joint Propulsion Conference & Exhibit* (Tucson, Arizona, 2005), p. 3856.

[16] Y. Hidaka, J. Foster, W. Getty, R. Gilgenbach, Y. Lau. J. Vac. Sci. Technol. A, **25**, 781 (2007). DOI: 10.1116/1.2746041

[17] B. Weatherford, J. Foster, H. Kamhawi. Rev. Sci. Instrum., **82**, 093507 (2011). DOI: 10.1063/1.3642662

[18] D.A. Bondarenko, K.V. Vavilin, S.A. Dvinin, I.I. Zadiriev, E.A. Kral'kina, I.A. Lobastov, S.Yu. Marinin, A.M. Nikonov, M.Yu. Selivanov. Prikl. Fiz., **3**, 11 (2022) (in Russian). DOI: 10.51368/1996-0948-2022-3-11-16

[19] A.S. Filatyev, A.A. Golikov, E.A. Kralkina, V.V. Sazonov, K.V. Vavilin. In *Proceedings of the 74th International Astronautical Congress (IAC)* (Baku, 2023), IAC-23-C4.9.7.

[20] Space Environment (Natural and Artificial) — Earth Upper Atmosphere. ISO/FDIS 14222, ISO 2013.

[21] Yu.P. Raizer. *Fizika gazovogo razryada* (Intellekt, Dolgoprudnyi, 2009) (in Russian).

[22] E.A. Kralkina, P.A. Nekludova, A.M. Nikonov, K.V. Vavilin, I.I. Zadiriev. Vacuum, **198**, 110873 (2022). DOI: 10.1016/j.vacuum.2022.110873

Translated by D.Kondaurov